CHARGING CONTROL TECHNIQUES*

R. E. Schmidt
General Electric Company

SUMMARY

Transparent conductive thin films of indium oxide and indium-tin oxide are evaluated for their properties to control charge buildup on satellite materials. Both oxide coatings are evaluated for their uniformity, stability, reproducibility and characteristics on various substrate materials such as FEP Teflon, Kapton, and glass.

Testing of the coated and uncoated satellite materials have been tested in 30cm square sizes. The materials performance have been characterized in multiple energy electron plasma environment and at low temperatures.

Grounding techniques for application to the coated multi-layer insulation (MLI) blanket designs and OSR arrays have been fabricated in the larger areas and tested under electron irradiation to evaluate their performance.

INTRODUCTION

The application of transparent conductive thin films to external spacecraft dielectric materials has been demonstrated on a small scale and shown to perform satisfactorily in simulated geosynchronous plasma charging environments. (Ref. 1) Several metal oxides have been evaluated using a number of deposition techniques including conventional vapor deposition, and RF and DC sputtering. Thin films of indium tin oxide (ITO) deposited using magnetron sputtering techniques has been found to provide the most stable conductive transparent coatings on spacecraft materials. Developmental work on coatings of indium oxide (IO) have also shown promise but have not been carried as far as the ITO. The work described in this paper represents some of the process development toward the optimization and characterization of these thin semiconductor oxide coatings and the evaluation on larger sizes performed for qualification for use on thermal control satellite materials

PROCESS DEVELOPMENT

The development efforts on the process characterization concentrated on

---

*This work was supported by the AFWAL, Materials Laboratory under Contract F33615-78-C-5119

determining the allowable variation in the process and coating parameters and still achieve highly transparent and conductive coatings on large sample sizes up to 30cm square. These process development characterizations considered deposition rate, reactive oxygen partial pressure and in situ biasing, coating thickness, uniformity, and a comparison between IO and ITO. This development has been evaluated in terms of the coating's solar absorptivity, surface resistance, stability of its shelf life, stability to tape and rub tests, and charge control performance under simulated substorm environements.

Thin conductive films of indium tin oxide (ITO) and indium oxide (IO) were evaluated on three types of substrates typical of external satellite dielectric materials. The materials considered were silvered and uncoated 125 μm (5 mil) FEP Teflon, aluminized and uncoated 75 μm (3 mil) Kapton and silvered and uncoated glass tiles. These materials represent flexible second surface mirror materials, external multilayer blanket insulation material, optical solar reflectors (OSR) and solar cell coverglasses.

The depositions of the semiconductor oxides onto the substrate materials were made by reactive magnetron sputtering in a Varian 3120H sputtering system using planetary fixture. The reactive deposit is accomplished by sputtering from the indium or indium-tin metal target in a partial pressure oxygen atmosphere. Magnetron sputtering has been found to be a cooler process as compared to conventional vapor deposition techniques. This is an important factor for depositions onto thermally sensitive materials such as Teflon.

Deposition Rate, Thickness

Best results were obtained by slowing the deposition rate down to about 1Å/sec and using an oxygen/argon gas flow ratio of about 1/3 to 1/4. The combination of the slower deposition and reduced oxygen partial pressure gave highly transparent films which were uniformly conductive across the 30cm square sheets of FEP Teflon and Kapton. The low deposition rate in combination with an in situ RF power applied to the sample holder resulted in an improved coating oxidation. Because of the relatively low melting temperature of the indium-tin target only about one percent of the available magnetron power was used during the deposition. Operation at higher power levels had the tendency to raise the temperature of the target and increase the probability of melting the metal target and electrically shorting the magnetron.

The oxygen/argon ratios were evaluated using a constant value for the oxygen flow rate of about 8cc/min into the chamber which corresponds to a partial pressure of about 53mN/m^2 (0.4m Torr.). Reactively sputtering at 1Å/sec, thickness of 200Å, 300Å, 500Å, 800Å, 1000Å and 5000Å were deposited during different runs with the deposition time being the only variable. All of the coatings were done with an in situ RF field of about 250 watts applied to the planetary fixture. 30cm square sheets of FEP Teflon, and Kapton and 12 one inch square tiles of microsheet were mounted onto the planetary during a typical run. Table 1 shows the relative surface resistance and optical properties of the ITO coatings as a function of coating thickness and oxygen/argon relative abundance. There does not appear to be a strong dependence between surface resistance and coating thickness. However, as the partial

pressure of oxygen flowing in the system is reduced, a definite increase in coating conductivity is observed, implying less oxidation and creation of a higher concentration of conduction electrons in the film. Furthermore, while the coating thickness had little effect on coating conductivity, the effect on the optical properties was more pronounced. Figure 1 shows the effect of the coating thickness on the spectral response of the transmittance through the coated microsheet. These values are for the higher resistance coatings in Table 1.

In addition to the SSM applications of the ITO, two coatings were applied to solar cell coverglass to evaluate their effect on cell performance. Figure 2a shows the I-V performance curve of the 2cm by 4cm solar cell before and after deposition of a 300A coating of indium tin oxide. The curves indicate about a 20% decrease in power at the peak power point. (.109 watt to 0.87 watt) as a result of the coating. The sheet resistance of the conductive coating was measured to be about 1KΩ/$\square$. The coverglass was bonded to the cell with Sylgard 182 and tested in a large area Pulsed Solar Simulation (LAPSS) facility.

Figure 2b shows the IV performance curves of a typical 2cm by 4cm solar cell before and after the deposition of a 100A thick ITO coating. The curves for the 100A ITO coated coverglass indicates about a 2% decrease in power at the peak point (0.005 watt to 0.113 watts). The transmittance of the 100A ITO coated coverglass was R = 0.120 and T = 0.868 for an absorptance of 0.01, an increase of less than 1% over the uncoated coverglass. This represents a significant reduction with coating thickness. The effect of the coating observed in both cells was primarily a decrease in the closed circuit current with little to no effect on the open circuit voltage.

Substrate

A definite dependence of the surface resistance on substrate material is shown in Table 2 with the harder substrates such as Corning 0211 microsheet glass having the highest conductive coatings, while the coatings on the FEP Teflon consistently had a high surface resistance for all of the thicknesses deposited. The amount of variation observed in the surface resistance of the indium tin oxide coatings on glass was found to be highly dependent upon the coating thickness and independent of the oxygen-argon settings. The typical standard deviations decreased from about 50% of the average value of the 100A coatings to about 10% for the 500A coatings. In contrast, the standard deviation in the surface resistance of the ITO coatings on the 75 μm (3 mil) Kapton was typically greater than 50% of the average value. Unlike the glass substrate, there was no consistent decrease in the variance with the thicker coatings on the Kapton. The FEP Teflon substrates showed a large variance in surface resistance in relation to the mean value reported in the Table. In all cases, the standard deviation of measurements across the 30cm samples was as large as and in some cases up to two times the average of the measured values.

IO vs ITO

Initial indium oxide (IO) coatings were deposited by reactive vapor deposition and showed significantly higher surface resistances compared to the ITO coatings deposited by magnetron sputter. They also required post deposition head treatment to improve the transparency of the deposited films. The increased oxidation during this post deposition treatment resulted in the increased transparency as well as, an increased surface resistance. It also produces the additional undesireable side effect of curling the edges of the polymer substrates, particularly on the FEP Teflon. Since reactive deposition of ITO from an indium-tin target was not attempted using resistive heating techniques, it was not clear whether the magnetron sputtering technique is a perferred technique or that ITO is a superior performance coating. Therefore, a similar process development was undertaken to evaluate indium oxide coatings. The initial coatings were applied in a thickness of 500A using an RF bias on the sample holder for improved coating oxidation and stability. Transparent conductive coatings were obtained using only slightly different deposition parameters (particularly the O_2/Ar ratio) than the ITO and required no post deposition heat treatment.

Because of the relative ease of using DC biasing techniques as compared to RF biasing, a DC Power source was used in place of the RF source. The result was that thin conductive transparent indium oxide coatings were deposited on microsheet, Kapton and FEP Teflon substrates with resulting electrical and optical properties as good as was obtained using the RF bias.

Substrates of glass and FEP Teflon were coated with thin coatings of IO and ITO in order to compare the two coatings in their optical and electrical properties in addition to their relative stabilities. The deposition of both oxides were made in thicknesses between 100A and 300A according to the quartz crystal monitor (QCM) which was set to their respective densities. Slightly different argon and oxygen flow rates and partial pressures were used to deposit the IO and ITO coatings. Both coatings were deposited using a DC bias on the sample planetary. It was found that in general, a slightly higher oxygen flow rate and partial pressure was necessary to deposit coatings of IO compared to the values required to deposit ITO coatings with similar optical and electrical properties. Table 3 summarizes the coatings which were made and their respective surface resistances which were measured immediately after the deposition.

The surface resistance of IO and ITO coatings from selective runs defined in Table 3 were remeasured after about four weeks. Comparison of measurements on coated samples from run numbers 1, 3, 5, 7, 10, 11, and 13 indicated similar changes in surface resistances for both IO and ITO coatings. In the case of the higher resistance ITO coatings (relative to the other values) deposited during runs number 1 and 3 resistance decreased by factors of 10 and 2 respectively, while for the other IO and ITO coatings the second surface resistance measurements were in general, 2 to 3 times higher. Therefore, both coatings seem to have comparable short term shelf life stability with comparable surface resistances for the same coating thickness.

QUALIFICATION TESTING

The materials testing discussed in this section cover a wide range of end-user concerns for application of the IO and ITO coated polymers and glass substrates. These include shelf life, humidity, thermal, vacuum, handling, grounding, ionizing radiation in addition to the performance under electron irradiation simulating the geosynchronous plasma environment.

Stability

Surface resistance and reflectivity measurements were taken on a group of IO and ITO coated samples which had been metalized on the back surface. For both the indium oxide and indium-tin oxide coatings, the surface resistances were in the range of 1 to 10kΩ/□ with the 300A coatings having the lower samples during the month of close evaluation.

Several large 30cm square samples of indium tin oxide and indium oxide coated Kapton and FEP Teflon which had been prepared early in the program were inspected and remeasured to determine their shelf life surface resistance. The coated samples came from two sets of depositions conducted in October, 1978 (ITO) and April, 1979 (IO). Surface resistance measurements were made across the 930cm^2 area of four sheets of the IO and ITO coated samples and the range of readings reported in Table 4. The values shows very little change in the surface resistance of both the IO and ITO coatings. All the materials had been kept between tissue paper to keep them clean and stored in large envelopes in open laboratory cabinets.

Humidity and Temperature

Another group of samples containing all six types of substrates and coatings were suspended over a large container which was partially filled with water. The container was then covered and placed in an oven which was maintained at a temperature of about 40°C. The reflectivity of the samples were measured after 3 days and are shown in Table 5. Additional measurements were not possible because of peeling of silvered backing on the glass and FEP samples. Surface resistance measurements on two sets of samples used in the humidity/temperature test are shown in Figure 4. The behavior of the coating surface resistance as a result of the higher temperature and humidity was found to be very dependent upon coating thickness and independent of the substrate. The curves indicate a large increase in the 100A coating compared to a high stability in the 200A and 300A thicknesses. The ITO exhibited larger variations than the IO coatings at the lower thickness. However, the variation in surface resistance during the two to three week exposure of all the coatings remained well within the allowable range for charge control surface properties.

Handling

A series of handling tests were performed on a 200A thick IO coated aluminized Kapton film. The tests were done to simulate several of the operations which the blanket material might experience during a typical

fabrication operation. A 30cm x 30cm sample was cut up into 2.5cm x 10cm strips for the purpose of this test. The magnetron sputtered coating had a surface resistance of about 2KΩ/□ . The results are shown in Table 6. The following discussion describes each test.

Crease Test - The strip was bent +180° with the IO coated side out. The crease was completed by pressing the bend together between the fingertips. The surface resistance was measured before and after the bend. A second strip was then creased in a -180° bend.

Tape Test - A 1.25cm wide Scotch Brand utility tape from 3M was pressed across the 2.5cm wide coated sample strip and removed. The surface resistance across the area was measured before and after the test. The tape was applied a second time and remeasured.

Rub Test - A 2.5cm wide strip of coated Kapton film was first rubbed with a dry Q-tip for about 10 seconds. A second test was performed with a wet Q-tip soaked in isopropyl alcohol.

Roll Test - A 2.5cm wide strip of coated Kapton was stretched with the coated side facing out over a 0.8cm diameter dowel with 180gm mass attached to the other side for tension. The strip was then slid over the dowel several times and the surface resistance measured periodically.

Thermal Cycle - A 2.5cm wide strip was alternately placed in a dewar of liquid nitrogen and removed and brought back to room temperature. The room temperature resistance of the coating was recorded after each LN_2 cycle.

Ionizing Radiation

The effect of ionizing radiation on the IO and ITO coatings were evaluated by placing 5cm wide strips of coated Kapton and FEP Teflon in a Gamma Cell model 220. The Cobalt 60 radiation source provided 1.7 and 1.33MeV photons at a flux of about 4.5Krads/min. Because of the ionizing effect of the radiation on air, the test was performed with the samples in a nitrogen gas purged cell. The radiation exposure was performed in 100 hour increments with visual inspection and surface resistance measurements between each increment. The samples were suspended between ends of an 8 inch diameter by 10 inch long cylindrical test cell and removed for each resistance measurement. Since FEP Teflon becomes brittle under this exposure, the surface resistance was measured in situ across the two ends through a piece of 1.25cm wide 3M conductive copper tape bonded to each end. Table 7 summarizes the coating performance after 700 hours of exposure. As seen from the data, the IO and ITO are stable under the ionizing radiation exposure.

Electron Irradiation

The characteristics of the larger uncoated and coated thermal control materials were tested in GE's large ESD test facility. The primary feature of this 1.3m diameter by 2.1m long vacuum test facility shown in Figure 5, is its dual beam electron flood gun capability. Each gun is capable of simultaneous irradiation of test specimens mounted at the opposite end of the chamber with electron energies from 0.5KeV up to 40KeV and at current densities in excess of $10nA/cm^2$ or as low as desired. The vacuum test facility uses a combination of cryogenics and turbomolecular pumping to achieve a nominal operating vacuum in the low $10^{-4}N/m^2$ (high 10^{-7} Torr) range.

The interior of the system is shrouded with a high permeability foil for reduced interference from external magnetic fields. The vacuum is monitored with an ion gauge which is turned off during measurements to prevent photo emission effects from the gauge filament. A viewing port on the side of chamber which is normally covered is used for sample viewing and photographic recording of any ESD phenomenon.

All test samples and diagnostics are mounted on the "swing away" door of the vacuum chamber. The platform for the samples and all diagnostics is a 91cm by 91cm grounded aluminum panel mounted on the inside of the chamber door. This allows for easy access to samples requiring complicated handling techniques. The 91cm square platform allows for simultaneous measurement of the performance of up to four 30cm square samples.

The diagnostics system was assembled to measure the charge control characteristics of flat 30cm square samples of conductively coated polymer films. The 30cm (1 foot) square samples are mounted to aluminum plates which are electrically isolated from the mounting table with Teflon spacers. A square aluminum ring is placed around the perimeter of the sample exposing a 29cm square. This electrode holds the sample in place and is used to measure any surface currents. A schematic of the sample configuration is shown in Figure 6. Keithley 410 picoammeters are connected between the back plate and surface ring and ground to measure displacement and surface currents. The schematic also shows the rotary arm whose axis is at the center of 91cm table. A Faraday cup mounted to a moveable carriage on the arm is used for measuring the current density across the sample. A Trek electrostatic surface voltmeter probe is also mounted on the rotary arm carriage for measuring surface potentials up to 20KV anywhere on the surface.

To provide a data base line for comparison with coated materials two 30cm (12") square uncoated sheets of 5 mil FEP Teflon and 3 mil Kapton were tested simultaneously under electron irradiation. The two samples were tested in an electron beam up to 16KeV at an average current density of about $2nA/cm^2$. Table 8 shows the surface and bulk currents and surface potentials as a function of incident electron energy. Surface discharges became so frequent at this current density above 16KeV that no additional measurements were made.

The surface potential of both materials rises nearly linearly with incident electron energy. The bulk currents of both materials increased significantly with respect to the surface current at the incident energies above 8KeV with the largest increases in the thinner Kapton. The discharge rates were not recorded for these measurements.

Another series of exposures of these two uncoated samples were made using both electron guns to show the charging control influence of the lower energy electrons. Each surface was irradiated for several minutes before steady state current readings and surface potential profiles were recorded. Table 9 summarizes these steady state measurements.

The variation of surface potential with incident electron energy or combination of energies shows the controlling influence of the lower energy

electrons when they are allowed to predominate. Not shown here is the long time constant and relative intensities required of the lower energy electrons to effectively discharge a precharged surface, particularly at the higher voltages.

In constrast to these currents and surface voltages 200A thick ITO coatings on 30cm squares of 75μm Kapton and 125μm FEP Teflon were tested under similar conditions of energy and density. The surface resistance of both samples were measured before mounting and were in good agreement with the values reported in Table 2. Table 10 summarizes the surface and conduction currents through the ITO coated materials. A change of direction in the bulk current was observed in the thin Kapton between 1 and 2KV due to the materials secondary emission variation over this voltage range. It should be noted that this reversal was not observed in the uncoated materials.

Similar measurements were recorded on 100A and 200A IO coatings with similar results. Following stabilization of the currents the Trek probe was swept across the samples while the beam was on. Before and after each sweep the probe calibration was checked over a grounded plate. No significant surface potentials were recorded in any of the measurements on any of the coated materials. Typically surface potentials of the coated polymers were below -10V during radiation and returned to zero when the beam was turned off.

GROUNDING

A 30cm X 30cm sheet of IO coated aluminized 50μm thick Kapton was used in the assembly of a conventional multilayer insulation (MLI) blanket to evaluate the utility of conventional blanket grounding techniques. The indium oxide coated Kapton had a surface resistance of about 2KΩ/□ across the transparent coating. The MLI covered with the transparent conductively coated aluminumized Kapton consisted of about 20 layers of alternating doubly aluminized 6μm (0.25 mil) thich mylar and dacron mesh.

The whole assembly was grounded with a Z shaped aluminum foil, which was laid in contact with each aluminized surface, on one edge of the blanket as shown in Figure 7a. The top flap of the Z foil aluminum strip was placed in contact with the indium oxide coating. At the bottom flap of the Z foil a strip of conductive metal velcro was attached. The whole assembly was then sewn together with a dacron thread. The grounding Z foil was about 5cm (2") in width. A similar Z foil was sewn on the same side but opposite corner of the blanket in order to facilitate hanging the blanket for subsequent ESD testing. This second Z foil used a standard cloth type velcro rather than the conductive hook used for ground. The strip of conductive metal velcro was attached to the top of the test sample holder shown in Figure 7b. The velcro was attached to the aluminum plate using Eccobond 57C and the blanket was suspended from the velcro strip. The surface ring with teflon tape on the back side to isolate it from the IO coating was placed over the blanket to prevent irradiation of the exposed blanket edges. The back plate sample holder and masking ring was then connected to ground through Keithley 410A picoammeters. In this configuration the resistance of the IO coating to ground was measured to be within 50KΩ to 75KΩ from anywhere on the top of the blanket.

The blanket assembly was then tested in an electron plasma with an average current density of about 0.5nA/cm^2. The electron energy was varied between 1KeV and 20KeV and the bleed off current from the IO coating to ground was recorded for several minutes at each energy level. The total bleed off current through the ground connection was approximately 0.5μA. The Trek electrostatic voltmeter probe was swept across the center of each sample after about 5 minutes of irradiation at each energy level while the electron plasma was still on. No surface potential above 10 volts was observed.

Two OSR arrays of uncoated and IO coated SSM tiles were tested in a 30cm X 30cm array to evaluate the scaled up grounding technique for the coated tiles.

These coated tiles were bonded to a 30cm square 1mm thick alodyned aluminum panel using RTV 566 and 567 loaded with 12% graphite fiber to provide a ground for the IO coating as shown in Figure 8a. A diluted SS 4155 primer was applied to both the aluminum and silvered microsheet OSR surface as is the usual procedure to improve the bonding strength. The average resistance between the top of the coated OSR and the aluminum panel was measured for all 144 tiles to the 44K with a maximum and minimum values of 410KΩ and 140Ω. The tiles were bonded to the aluminum panel using standard vacuum bagging techniques for a uniform pressure application. The 12 by 12 array of IO coated and silvered 0211 glass tiles were mounted in the ESD facility along with a 12 by 12 array of uncoated silvered 0211 galss. The uncoated array was also bonded to an aluminum panel with graphite fiber loaded RTV 566 adhesive. Figure 8b shows the placement of the two OSR panels in the chamber. An aluminum ring insulated on the back was placed over the samples for holding them in contact with the back plate used to measure the ground current. The surface ring was also attached to ground. One row of glass tiles along an edge of the uncoated array was unsilvered in order to evaluate the possible effect of any discharges or current through the glass on the bond with the conductive adhesive.

The samples were irradiated simultaneously by electrons between 1KeV and 16KeV at current densities of about 1nA/cm^2. Higher energies were not used due to incidence of violent discharge on the uncoated sample. Table 11 summarizes the measured currents and maximum surface potential from the two samples. The measured surface potential on the uncoated array during the 16KeV irradiation is lower than that measureed during the 12KeV irradiation, due to the large fluctuations in the surface potentials occurring during the larger discharges. The notation on the uncoated ground currents illustrate the increasing discharges both in magnitude and frequency with increasing electron energy. The surface potential on the array of IO coated OSR's never exceeded 10 volts negative.

CONCLUSIONS

Highly stable, low resistance, low absorptance thin coatings of indium-tin oxide and indium oxide have been successfully and repeatedly deposited on flexible and glass thermal control spacecraft materials. Reactive magnetron sputtering from a metal alloy target has been shown to provide very repeatable depositions. The results show that optimum transmission and

solar reflectance and performance in a radiation environment can be obtained only by minimizing the coating thickness. The optimal thickness for a particular application must be determined by balancing the deposition capability and handling characteristics with a resistivity and solar abosrptivity stability sufficient to achieve charge control.

Storage, handling and environmental testing indicate that 200A coatings can be reproducibly deposited and provide highly stable semiconducting properties with solar absorptances of less than two percent The coatings applied to glass, FEP Teflon and Kapton substrates can be tailored to the low kilohm/square range. Because of the nature of the sputtering process, particularly for non-dedicated systems, exact values of the process variables cannot be specified. However, the general dependence between the process variables and coating properties have been established.

All radiation measurements of the coatings under simulated substorm conditions have exhibited the characteristics of stable charge control. Measurements of surface potentials during and after irradiation by electrons up to 30KeV and ionizing gamma radiation show an effective stable grounding surface.

REFERENCES

1 Eagles, A. E., Amore, L.J., Belanger, V.J., Schmidt, R. E.; Spacecraft Static Charge Control Materials; AFML-TR-77-105, Part II, 1978.

2 Schmidt, R. E., Charging Control Satellite Materials: AFWAL-TR-80-4017, Part I, 1980.

TABLE 1. COMPARISON OF COATING THICKNESS AND O_2 RELATED PRESSURE

DEPOSITION THICKNESS o (A)	OXYGEN/ARGON FLOW RATE							
	8/24				8/28			
	R	T	A	SURF. RES. (KΩ)	R	T	A	SURF. RES. (KΩ)
200	.14	.82	.04	530	.12	.87	.01	9.1
300	.17	.78	.05	1900	.18	.80	.02	6.4
500	.17	.77	.06	127	.17	.76	.07	2.1
800	.17	.77	.06	5600	.15	.76	.09	1.3
1000	.15	.77	.08	735	.15	.77	.08	4.0
5000	.13	.71	.16	70	.14	.71	.15	11.2

Table 2 Average Surface Resistance of ITO Coated Substrates

Thickness o (A)	Oxygen: Argon Flow Ratio = 1:35			Oxygen: Argon Flow Ratio = 1:4		
	Glass	Kapton	FEP Teflon	Glass	Kapton	FEP Teflon
100	331	1330	207×10^3	4.7	292	14.3×10^3
	59	2960	10^6	11.0	65	8.8×10^3
200	8.5	532	13×10^3	1.1	10	6.7×10^3
	6.4	492	7.8×10^3	1.5	31	10.8×10^3
				2.1	340	12.7×10^3
300	1.22	134	3.3×10^3	1.2	26	3.1×10^3
	0.84	304	2.23×10^3	1.0	299	2.9×10^3
500	1.53	633	4.8×10^3	0.54	8.0	5.4×10^3
	1.47	88	6.1×10^3	0.72	5.0	1.5×10^3

TABLE 3. IO AND ITO COMPARISON

RUN #	SUBSTRATE	SIZE (cm x cm)	THICKNESS (Å)	COATING	SURFACE RESISTANCE (Ω)
1	Glass	2.5 x 2.5	100Å	ITO	140 K
	FEP Teflon	2.5 x 5	100Å	ITO	9 Meg
2	FEP Teflon	15 x 15	100Å	ITO	500 K - 5 Meg
3	Glass	2.5 x 2.5	200Å	ITO	20 K - 100 K
	FEP Teflon	2.5 x 5	200Å	ITO	30 K - 40 K
4	FEP Teflon	15 x 15	200Å	ITO	20 K - 80 K
5	Glass	2.5 x 2.5	300Å	ITO	3 - 3.5 K
	FEP Teflon	2.5 x 5	300Å	ITO	5 K
6	FEP Teflon	15 x 15	300Å	ITO	3 - 10 K
7	Glass	2.5 x 2.5	100Å	IO	12 - 18 K
	FEP Teflon	2.5 x 5	100Å	IO	65 - 140 K
8	Glass	2.5 x 2.5	100Å	IO	14 K
	FEP Teflon	2.5 x 5	100Å	IO	80 K
9	FEP Teflon	15 x 15	100Å	IO	35 K - 85 K
10	Glass	2.5 x 2.5	200Å	IO	4 - 6 K
	FEP Teflon	2.5 x 5	200Å	IO	6 - 10 K
	FEP Teflon	15 x 15	200Å	IO	8 - 16 K
11	Glass	2.5 x 2.5	300Å	IO	1.2 K
	FEP Teflon	2.5 x 5	300Å	IO	1.5 K
12	FEP Teflon	15 x 15	300Å	IO	.9 - 1.5 K
13	Glass	2.5 x 2.5	500Å	IO	.5 - .7 K
	FEP Teflon	2.5 x 5	500Å	IO	.4 - .5 K
14	FEP Teflon	2.5 x 5	500Å	IO	.4 - .7 K

TABLE 4. LONG TERM ITO AND IO COATING STABILITY

SUBSTRAT	COATING	THICKNESS (A)	INITIAL Rs (KΩ)	SHELF LIFE (Months)	SURFACE RESISTANCE (KΩ)
KAPTON	ITO	100	10	22	10-50
		200	20	22	20-490
KAPTON	IO	100	15	16	3-5
		100	8	16	3-8
FEP TEFLON	ITO	100	1.4×10^4	23	$3 \times 10^4 - 2 \times 10^6$
		200	1.2×10^4	23	$1 - 2 \times 10^6$
FEP TEFLON	IO	100	$2 - 50 \times 10^4$	17	$7 \times 10^4 - 30 \times 10^4$

TABLE 5. COATING STABILITY UNDER HUMIDITY TEST

Coating	Substrate	Coating Thickness (Å)	REFLECTIVITY	
			Initial	3 Days of Humidity
ITO	Glass/Ag	0	0.92	-
		100	0.90	0.88
		200	0.88	-
		300	0.86	0.84
	FEP/Ag	0	0.86	
		100	0.86	0.85
		200	0.82	-
		300	0.80	0.82
	Kapton/Al	0	0.37	
		100	0.37	
		200	-	
		300	0.35	
IO	Glass/Ag	0	0.92	-
		100	0.86	0.85
		200	0.84	-
		300	0.81	0.79
	FEP/Ag	0	0.86	-
		100	0.81	0.82
		200	0.78	-
		300	0.76	0.76
	Kapton/Al	0	0.37	
		100	0.37	
		200	0.34	
		300	0.29	

TABLE 6. IO COATING HANDLING TESTS

TEST	PRE TEST RESISTANCE (K Ω)	POST TEST RESISTANCE (K Ω)
CREASE +180°	3	1.5×10^6
CREASE -180°	5	330
TAPE 1st	2	4
TAPE 2nd	4	6
RUB-DRY	2	9
RUB 1st WET	3	22
RUB 2nd WET		70
ROLL 3	2.5	3.0
10	--	3.2
20	--	3.8
THERMAL CYCLE 1	3	3
2	--	3
3	--	3

TABLE 7. IONIZING PHOTON* EXPOSURE

EXPOSURE (10^7 RAD)	IO/KAPTON (K~)	ITO/KAPTON (K~)	ITO/FEP (K~)
0	0.62	5.16	625
2.7	0.53	1.68	340
5.4	0.48	1.47	2400
8.1	0.45	1.18	4500
10.7	0.51	2.22	2100
13.4	0.50	1.32	3200
16.1	0.50	1.18	
18.7	0.47	1.39	

* Cobalt 60-γ

TABLE 8 UNCOATED FLEXIBLE SUBSTRATE PERFORMANCE UNDER MONOENERGETIC IRRADIATION

ACCELERATING VOLTAGE (K.V)	TEFLON (5 MIL)				KAPTON (3 MIL)			
	PLATE CURRENT (nA)	SURFACE CURRENT (nA)	SURFACE VOLTAGE MIN (V)	SURFACE VOLTAGE MAX (V)	PLATE CURRENT (nA)	SURFACE CURRENT nA	SURFACE VOLTAGE MIN (V)	SURFACE VOLTAGE MAX (V)
1	43	31	0	-11	23	95	-17	-39
2	68	135	-42	-154	30	244	-775	-998
3	18	88	-900	-1140	28	170	-1450	-192
4	14	92	-1738	-2065	22	157	-2400	-2925
5	15	110	--	-3090	24	175	-3300	-4020
6	14	96	-3550	-4000	26	155	-4200	-4960
7	11	100	-4380	-4870	22	152	-4800	-5730
8	15	99	-4850	-5730	38	152	-5270	-6500
10	28	105	-6570	-7800	80	148	-6950	-8420
12	48	102	-7780	-9240	140	143	-7560	-9390
14	48	105	-9300	-10980	167	145	-8230	-9840
16	59	100	-10970	-12480	200	142	-8790	-10770

TABLE 9 UNCOATED FLEXIBLE SUBSTRATE PERFORMANCE UNDER MULTIPLE ENERGY IRRADIATION

RUN #	GUN	V_{ACC} (kV)	I_{INC} (nA/cm²)	FEP TEFLON/Ag			KAPTON/Al		
				I_B (nA)	I_S/I_B	V_S (V)	I_B (nA)	I_S/I_B	V_S (V)
1	1	1	0.8	6.0	0.42	-6	24.5	0.15	-27V
2	2	1KV	0.8	7.5	1	-6	48.0	0.17	-72
2A	2	2kV	0.8	5.2	4.1	-324	17.0	1.1	-914
3	1	2KV	0.8	3.1	4.0	-377	7.2	0.75	-976
4	1	2KV	1.9	15.8	1.0	-10	88	0.44	-176
	2	1KV							
5	1	3KV	1.9	17.0	1.4	-24	92	0.38	-249
	2	1KV							
6	1	3KV	0.8	2.3	5.9	-1486	5.9	1.8	-1950
7	1	3KV	2.6	28.2	0.9	-1478	45.5	0.38	-1916
	2	1KV							
8	1	3KV	0.8	1.95	5.4	-1478	4.8	2.1	-1911
9	1	3KV	1.5	5.8	6.2	-759	18.5	1.6	-1080
	2	2KV							
10	1	1	0.8	3.5	0.6	-6	17.4	0.16	-8
11	2	1	0.8	6.5	0.94	-8	40	0.17	-9
12	1	2	0.8	3.3	4.2	-485	14	0.51	-866
13	1	2	1.4	13.4	0.86	-9	69	0.36	-85
	2	1							
14	1	4	1.4	15	1.1	-72	79	0.37	-130
	2	1							
15	1	5	1.5	17.5	1.2	-117	90	0.47	-136
	2	1							
16	1	4	0.8	3.5	3.9	-2610	41	0.23	-2868
17	1	5	0.8	4.3	3.4	-3521	40	0.23	-3742

TABLE 10 SUMMARY OF CURRENT MEASUREMENT ON ITO COATED KAPTON AND FEP TEFLON FLIMS

Beam Voltage (kV)	ITO/Kapton (75 μm)		ITO/FEP Teflon (12.5 μm)	
	Surface Current (nA)	Bulk Current (nA)	Surface Current (nA)	Bulk Current (nA)
1	720	-75	28	32
2	230	52	36	25
3	270	48	40	18
4	800	37	55	13.5
5	1200	29	84	10
7.5	1500	26	110	7.6
10	1600	25	125	7.3
15	1650	24	150	7.8
20	1700	24.5	170	8.8
30	1800	26	210	10.5

TABLE 11 PERFORMANCE CHARACTERISTICS OF 12" X 12" OSR ARRAY

ACCELERATING POTENTIAL (KV)	INCIDENT FLUX (nA/cm^2)	UNCOATED		COATED (200A IO)	
		GROUND CURRENT (nA)	SURFACE POTENTIAL (V)	GROUND CURRENT (nA)	SURFACE POTENTIAL (V)
1	1.3	27	-30	89	-15
2	0.9	52	-35	187	-10
3	1.1	355	-280	249	-15
4	1.0	305	-950	240	-10
6	1.3	360	-2425	330	-10
8	1.2	395	-4000	375	-10
10	1.0	335[+]	-6050	360	-10
12	1.1	370[++]	-7750	420	-10
16	1.3	560[+++]	-6500	460	-10

[+]10 DISCHARGES/90 SEC (4:10-40nA; 6: 40-50nA)

[++] 9 DISCHARGES/90 SEC (5:10-50nA; 4: 50-100nA)

[+++]27 DISCHARGES/90 SEC (21: 10-50nA; 5: 50-100nA, 1: 100-200nA)

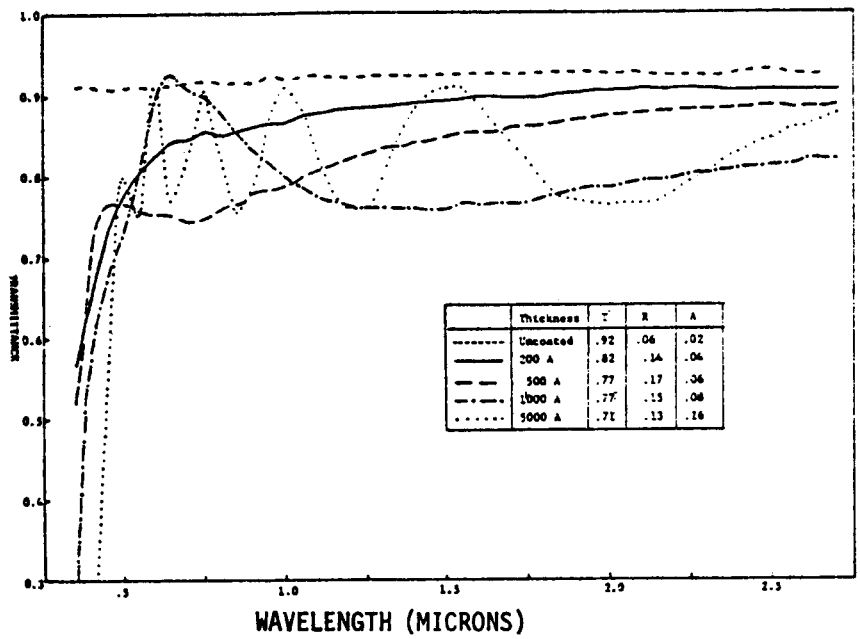

Figure 1. - Transmittance of ITO-coated microsheet.

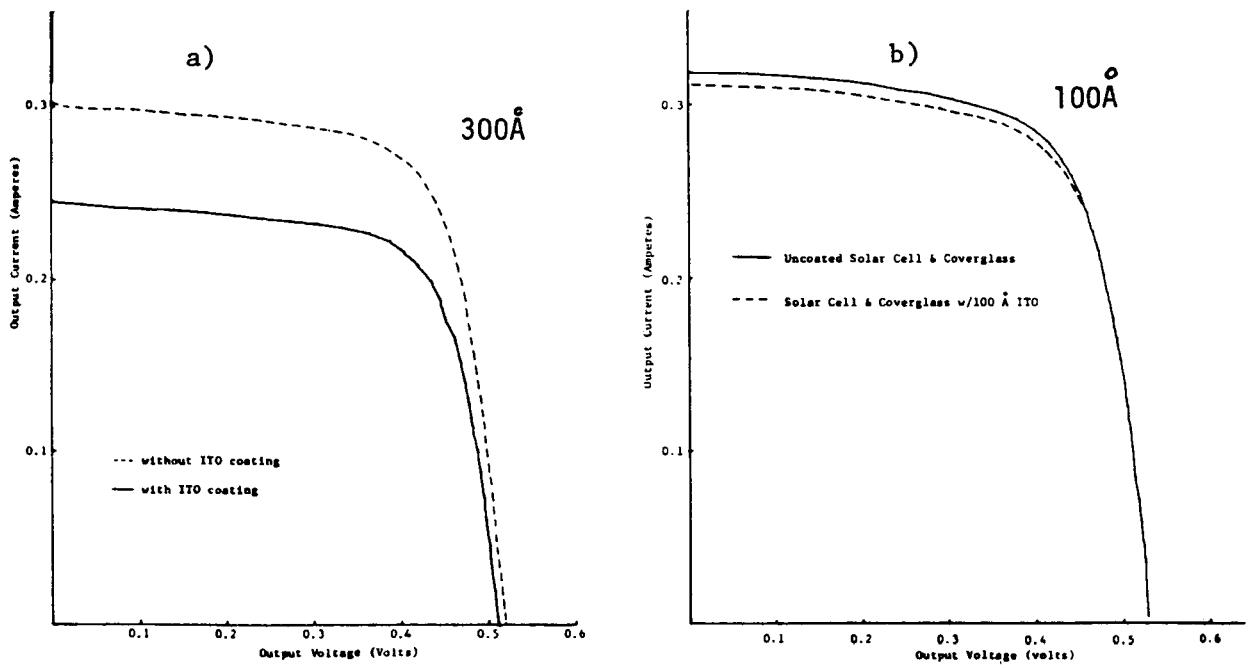

Figure 2. - IV curve of 2-cm x 4-cm solar cell with ITO-coated coverglass.

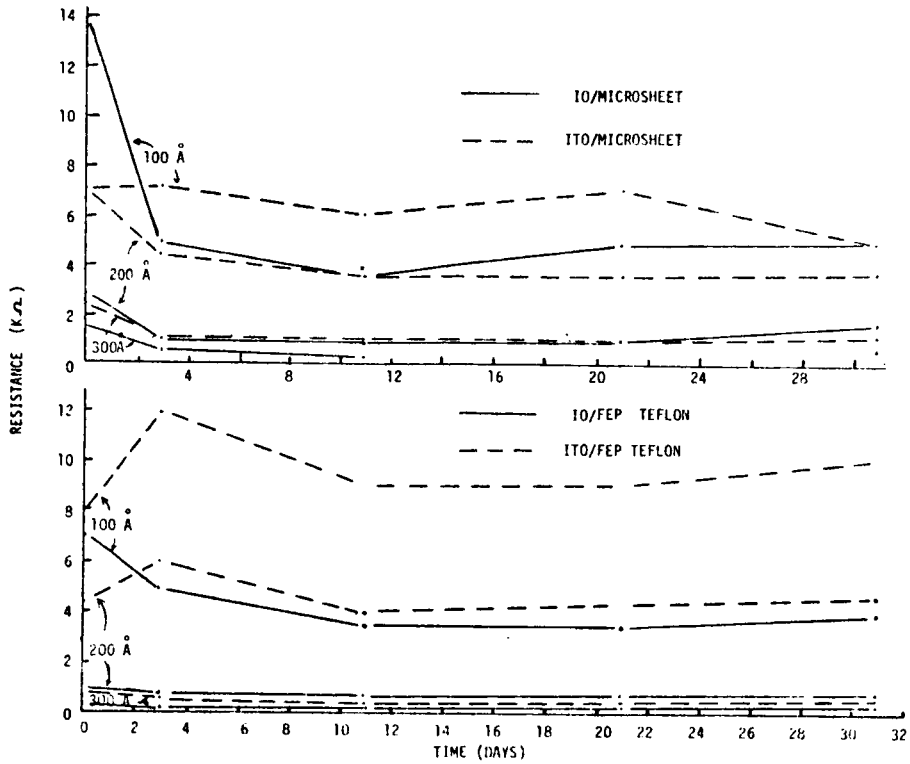

Figure 3. - Surface resistance stability of reference samples.

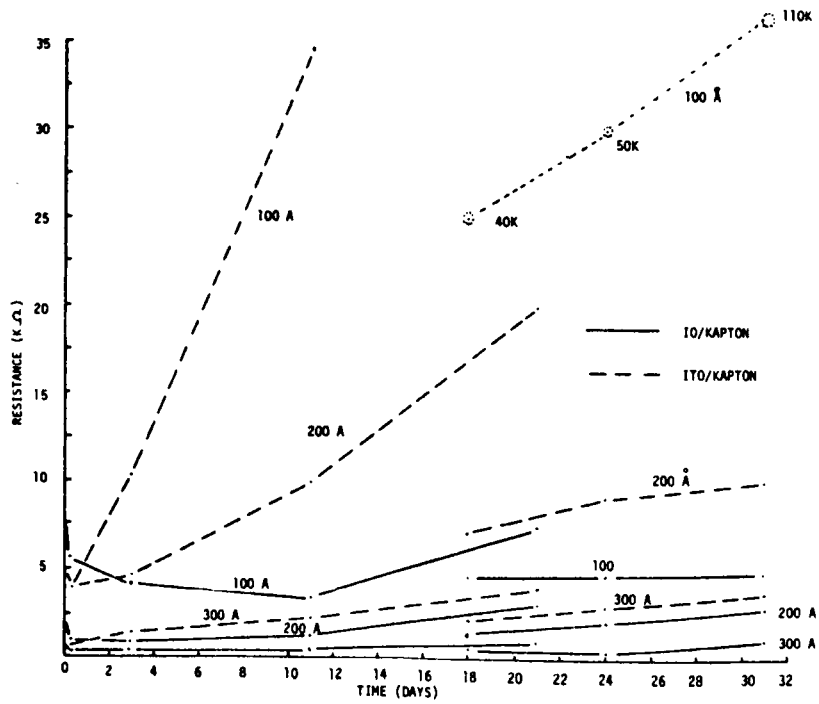

Figure 4. - Typical surface resistance variation during humidity test (Kapton).

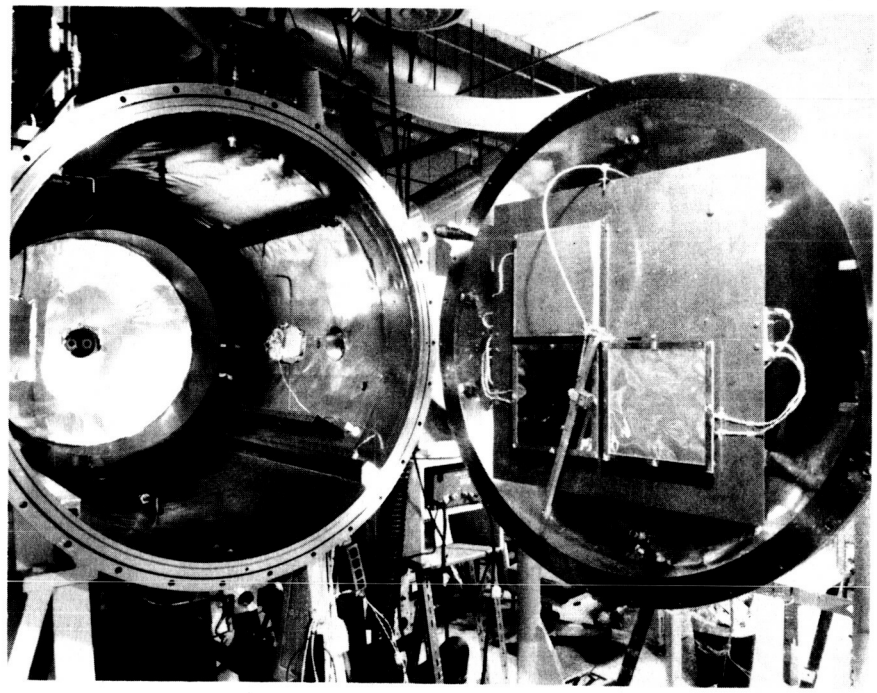

Figure 5. - Sample configuration in test chamber.

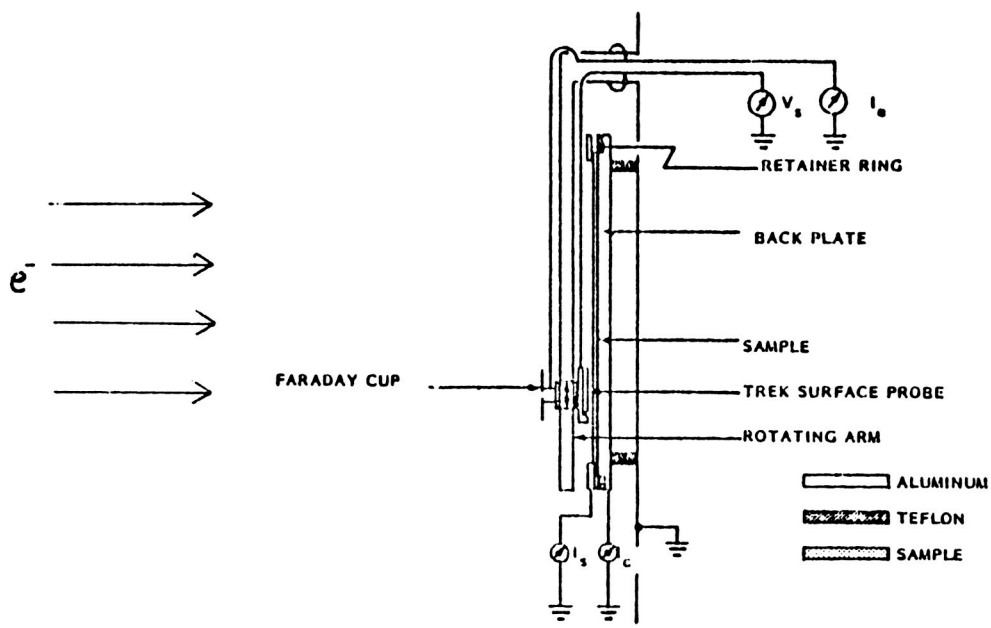

Figure 6. - Sample test configuration.

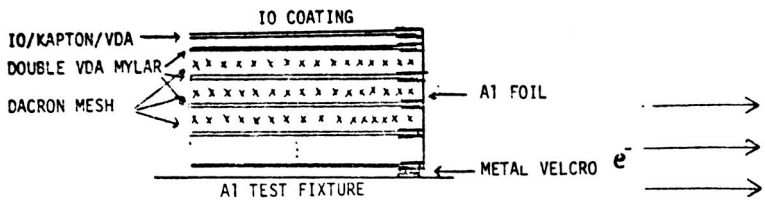

Figure 7a. - MLI blanket grounding.

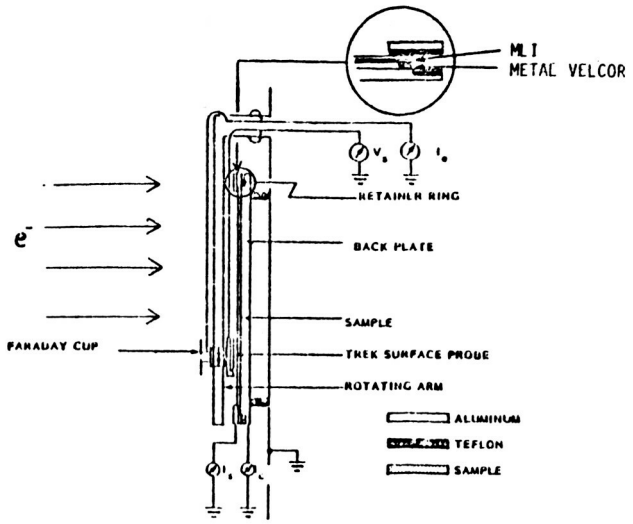

Figure 7b. - Schematic of sample configuration.

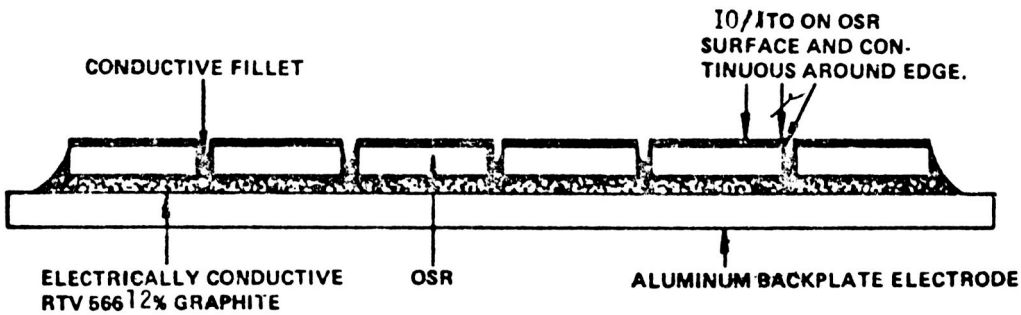

Figure 8a. - Coated OSR array grounding.

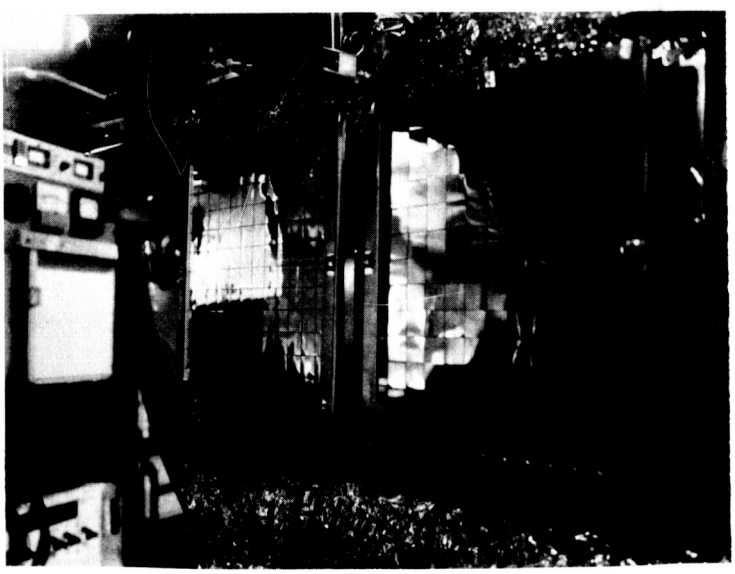

Figure 8b. - Actual OSR test configuration.